Article submitted to: High Power Laser Science and Engineering, 2025 *July 30, 2025*

Active control of the laser beam pointing for the Zettawatt-Equivalent Ultrashort pulse laser System: A proof-of-principle study with 16-inch optics

Hao Huang[1], Tanner Nutting[1], Andrew McKelvey[1], Bixue Hou[1], Miloš Burger[1], Yong Ma[1], Lauren Weinberg[1], Galina Kalinchenko[1], Anatoly Maksimchuk[1], John Nees[1], and Karl Krushelnick[1]

[1]*Gérard Mourou Center for Ultrafast Optical Science, University of Michigan, Ann Arbor, MI 48109, USA*

Abstract

We present a proof-of-principle study of active beam-pointing control for the Zettawatt-Equivalent Ultrashort pulse laser System (ZEUS) using a piezo-actuated 16-inch mirror. To the best of our knowledge, this is the largest actively controlled mirror reported in a high-power laser system. A simple proportional feedback control was implemented based on a field-programmable gate array (FPGA), which reduced the standard deviation of beam-pointing fluctuations by 91% to 0.075 μrad in the horizontal direction and by 78% to 0.25 μrad in the vertical direction. We also demonstrated the elimination of long-term pointing jitter caused by temperature drift using the same apparatus.

Keywords: Laser pointing control; tip/tilt mirror; proportional feedback control; piezoelectric actuator

1. Introduction

The rapid development of ultrafast and ultra-intense laser systems opens a new path to extreme conditions in the laboratory, such as ultrafast time scales, ultra-intense electromagnetic fields, and ultra-high energy densities, which are of significant interest to research into ultrafast molecular dynamics[1], laboratory astrophysics[2,3], laser-driven nuclear physics[4,5], laser-plasma accelerators[6–14] as well as strong-field quantum electrodynamics (SF QED)[15,16]. Tightly focused high-peak-power laser pulses with intensity exceeding 10^{18} W/cm^2 also open new horizons in the relativistic optics regime. For many applications, the preferred extreme intensity greater than 10^{22} W/cm^2[17,18] or even 10^{23} W/cm^2[19] is only obtainable within a micrometer-sized focal spot. Therefore, taking full advantage of these lasers' extreme intensity at focus requires precise control of the laser beam pointing.

The construction of the Zettawatt-Equivalent Ultrashort pulse laser System (ZEUS) at the University of Michigan will enable flagship experiments designed to collide a high-energy electron beam from a laser wakefield accelerator (LWFA) with a focused ultrashort laser pulse[20,21]. Such an experiment would enable the study of the new physics in SF QED via two basic processes, i.e., multi-photon Compton scattering and multi-photon Breit-Wheeler pair-production, in the collision of high-energy electrons and high-intensity laser pulses[22–24]. The designed diameter of the electron beam at the interaction point is less than 100 μm. Consequently, the positional deviation of the focused laser pulse must be within this range so that the interaction between them can be realized. This requires both the wakefield-driver laser and the colliding laser to have minimal beam-pointing instabilities (< a few μrad). Besides the colliding experiment, the production of relativistic electron beams with narrow energy spread through LWFA would also benefit from a pointing-stabilized high-power laser[25–27], in addition to enabling a wide variety of temporally-resolved pump-probe experiments.

Correspondence to: Hao Huang. Email: haohg@umich.edu

2. Theoretical Background

To control laser beam pointing, a fast tip/tilt mirror is often employed rather than a deformable mirror. Due to the relatively low laser-induced damage thresholds of optical coatings (a few J/cm^2), large-diameter beams and, consequently, mirrors with large apertures are required in high-power laser systems. To preserve the surface flatness, the minimum thickness of a large-aperture optic scales with its aperture (d). As a result, the mass of such optics scales as the cube of the optical aperture.

The natural frequency of a mechanical system on its ith

10.1017/hpl.2025.10064
https://doi.org/10.1017/hpl.2025.10064 Published online by Cambridge University Press

degree of freedom can be depicted as[28]:

$$f_i = \frac{1}{2\pi}\sqrt{\frac{K_i}{J_i}}\,, \tag{1}$$

where K_i and J_i denote the stiffness and inertial mass on its ith degree of freedom. Eq. 1 illustrates the bandwidth limitation of large-aperture, tip/tilt mirrors, as their natural frequencies are inversely proportional to their aperture (to the power of -3/2). Two approaches could be pursued to improve a tip/tilt mirror's bandwidth: increasing the stiffness or decreasing the inertial mass. The first approach usually involves a comprehensive design, finite element analysis (FEA), and customization of rigid flexures[29,30]. The latter could be achieved using lightweight materials and the use of complex structures such as honeycombs[31].

The above-mentioned aperture-bandwidth dilemma for tip/tilt mirrors has been posing significant challenges for the high-power laser community as well as for applications of these lasers. In fact, most actively controlled tip/tilt mirrors or mechanisms reported in the literature[32–38] or which are commercially available[39] are limited to ∼4 inches in diameter. Although large-aperture tip/tilt mirrors are widely used in astronomical telescopes[31], their high cost, heavy weight, and large footprint make them less attractive candidates for use in table-top high-power laser systems in academic or industrial laboratories.

3. Design Considerations

The aim of this investigation is to develop a cost-effective, compact, large-aperture, fast tip/tilt mirror that would mainly utilize off-the-shelf components to enhance the pointing stability of a very high-power laser system. The positional stability of the collimated ZEUS laser beam is sufficient to avoid beam clipping; however, pointing stability improvements such as those demonstrated in this work can significantly enhance the viability of colliding experiments that depend on control of the focal spot location. Several considerations were carefully weighed during the design phase, including employing a low-profile design to accommodate the 12-inch beam's height from upstream and maintaining the ability to detect the beam leakage through the mirrors. Mechanical simulations were conducted to enhance the stiffness-to-mass ratio of the mirror in the horizontal and vertical directions, thus increasing the mirror's resonance frequency (Eq. 1).

In this work, we present a proof-of-principle study of actively controlling a 16-inch mirror assembly by sampling a continuous-wave (CW) laser diode output at 100 Hz, which effectively resembles the regenerative amplifier of the ZEUS laser operating at the same repetition rate. It has been demonstrated that the low-power, unamplified pulse train from the front-end of a laser system (100 Hz for the ZEUS laser) carries the same beam-pointing properties as the high-power, fully-amplified pulses (1/60 Hz for the ZEUS laser) originated from the same front end[35]. As a result, actively controlling the beam pointing of the unamplified pulses within the 100-Hz pulse train leads to optimized pointing stability of the fully amplified beam (selected pulses from the same 100-Hz pulse train) at the focus. A simple proportional feedback control was implemented to serve this purpose. For industry-standard proportional-integral-derivative (PID) control algorithms, the correcting signal output $u(t)$ as a function of the error signal input $e(t)$ can be expressed as $u(t) = K_P e(t) + K_I \int e(t)\mathrm{d}t + K_D \frac{\mathrm{d}e(t)}{\mathrm{d}t}$, where K_P, K_I, and K_D are the proportional, integral, and derivative coefficients, respectively. In this work, only the first proportional term is taken into account for simplicity and baseline timing study; thus, the correcting signals driving the piezo-actuators $u(t) = K_P e(t)$. The error signal input $e(t)$ is generated by a position sensing detector, which monitors the position of the focal spot's centroid.

4. Design Overview

Actuating such a large optic is critical due to the requirement for independent control of the 12-inch laser beam pointing after the final amplifier for the colliding experiment discussed above. Therefore, we implemented a simple proportional feedback control and observed reductions of the standard deviation of beam-pointing fluctuations by 91% and 78% in the horizontal and vertical directions, respectively. Although the geometrical and mechanical properties of the fast tip/tilt mirror were tailored to meet the ZEUS laser's requirement, other high-power laser facilities can easily adopt this study's principles to improve beam-pointing stability. To the best of our knowledge, this work features the largest actively controlled optic used in a high-power laser system.

The optics used in this work have a diameter of 16 inches and a thickness of 2 inches. They have a broadband, high-reflective coating on their front surfaces designed for maximum reflectivity at an incident angle of 22.5°. Up to 120-J, 1-ns duration amplified pulses would be steered 90° by the 16-inch mirrors and enter into the 3-PW compressor of the ZEUS laser[20,21]. As shown in Fig. 1(c), the amplified beam is reflected by the original 16-inch mirror with only manual tip/tilt adjustment, followed by the 16-inch fast tip/tilt mirror with piezo-actuators. The original 16-inch mirror assembly was based on an off-the-shelf rotation stage driven by a high-precision adjustment screw and a micrometer-driven tilt platform (Newport Corporation) to realize the manual tip/tilt adjusting mechanism with low profile. It also consists of a custom stainless steel V-block, a reinforcement block, and a thin steel strap to rigidly mount the optics, as shown in Fig. 1(a). The total assembly weighs ∼50 kg. We implemented two measures to increase the resonance frequency of such heavy assembly through enhancing its stiffness-to-mass ratio (Eq. 1). A flat fused

https://doi.org/10.1017/hpl.2025.10064 Published online by Cambridge University Press

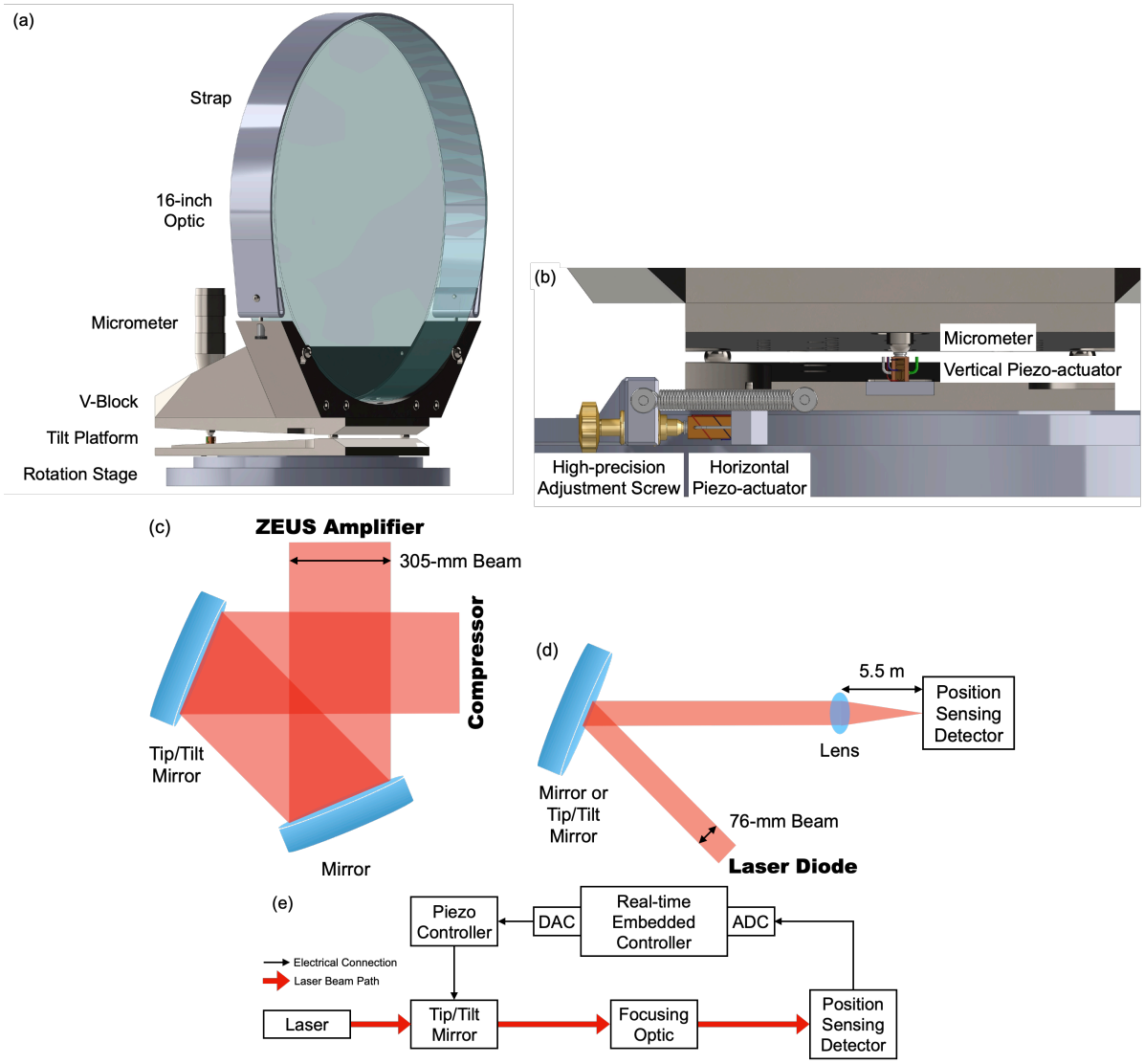

Figure 1. Experimental setup. (a) Computer-aided design (CAD) model of the 16-inch mirror assembly. (b) Enlarged view of the horizontal and vertical piezo-actuators. (c) Beam path of amplified ZEUS laser beam turning 90° by two 16-inch mirrors. (d) Beam path of 16-inch mirror testing setup using laser diode (not to scale). Mirror: original 16-inch mirror assembly without piezo-actuators. Tip/tilt mirror: piezo-actuated 16-inch mirror assembly. (e) Schematic of the active control of laser beam pointing.

silica substrate assures the stiffness of the optic and allows beam leakage, compared to a hollowed substrate. The optic is held onto the V-block through the thin steel strap to avoid excess weight around the top portion of the mirror.

The 16-inch fast tip/tilt mirror assembly with two piezo-actuators (PC4QMC2, Thorlabs, Inc.) installed against the adjustment screw and micrometer was constructed to demonstrate active control of beam pointing. A modular design was adopted such that the two piezo-actuators with adapter plates could be easily installed or de-installed (Fig. 1(b)). The piezo-actuators have a maximum displacement of ∼9 μm and 1000 N of blocking force. The calculated resonant frequency of the piezo-actuators under the mechanical load is around 1 kHz. The two piezo-actuators were carefully aligned and centered with the adjustment screw and micrometer to avoid excessive tensile stresses that would lead to their failure. The positions of the piezo-actuators were then fixed with high-temperature epoxy during the first installment.

5. Experimental Setup

To study the effects of the ambient environment on the beam-pointing stability, we also employed an apparatus to characterize vibration and temperature simultaneously. Two high-sensitivity, three-dimensional seismic accelerometers (356B18, PCB Piezotronics, Inc.) synchronously measured the vibration on the laboratory floor and the optical table. The accelerometer has a resolution of 5×10^{-5} g with a frequency range (±5%) covering 0.5 to 3000 Hz. We precisely aligned the x-axis and y-axis of the accelerometers

https://doi.org/10.1017/hpl.2025.10064 Published online by Cambridge University Press

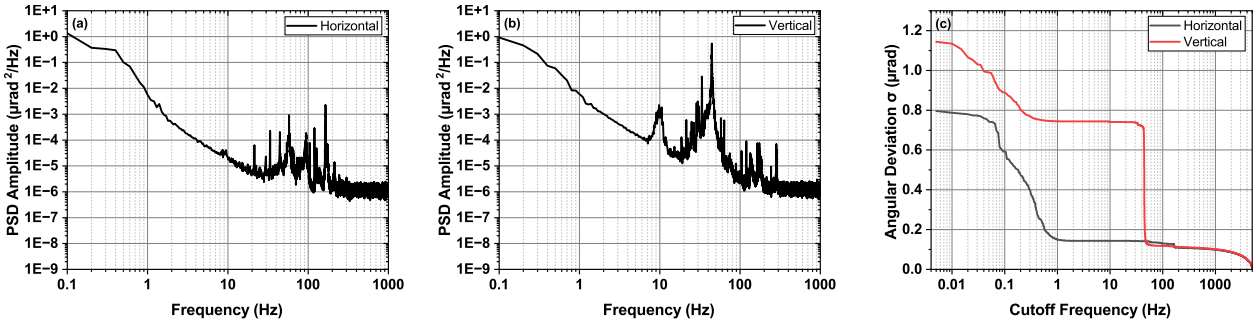

Figure 2. Short-term characterization of the original 16-inch mirror assembly. PSD: power spectral density. (a) Power spectral density of horizontal angular deviation. (b) Power spectral density of vertical angular deviation. (c) Comparison of the standard deviation of horizontal (black) and vertical (red) angular pointing fluctuations, with only frequencies higher than the cutoff frequency contributing to the standard deviation.

along the directions perpendicular and parallel to the optical table chain, and their z-axis vertically with respect to the optical table surface[21]. A temperature logger with 0.024°C resolution was placed on the optical table adjacent to the 16-inch mirror assembly to record the temperature every minute.

While waiting for the construction of the Ti:sapphire laser beam to be complete, we performed a proof-of-principle study of active beam-pointing control using a CW laser diode at 808 nm (Fig. 1(d)). By sampling the CW beam only at 100 Hz, we effectively simulated the operation of the active control system with the Ti:sapphire regenerative amplifier outputs at 100 Hz. The single-mode, polarization-maintaining CW fiber output was first collimated to a 3-inch diameter beam. The collimation and beam profile were verified using a wavefront sensor. The collimated 3-inch beam was then incident on the top portion of the 16-inch mirror assembly (original or piezo-actuated mirror) at 22.5°, and the reflected beam was focused with a lens with a 5.5-m focal length. A two-dimensional, lateral effect position sensing detector (PDP90A, Thorlabs, Inc.) was placed at focus to measure the position of the beam's centroid. The detector has a bandwidth of 15 kHz and is capable of resolving 0.75-μm displacements, corresponding to an angular resolution of 0.14 μrad. The laser diode, focusing lens, and position sensing detector were rigidly mounted on the chain of optical tables holding the ZEUS laser system[21]. The beam-pointing instability induced by these three elements is determined to be negligible (∼0.1 μrad) compared to that induced by the 16-inch mirror in a baseline study.

A simple proportional feedback loop was realized in the onboard field-programmable gate array (FPGA) of a real-time embedded controller (CompactRio, National Instruments), which acquires the position sensing detector outputs as the feedback loop's error signal inputs and produces the corrected voltage to drive the piezo-actuator. The proportional coefficient K_P was carefully adjusted to minimize the standard deviation of angular beam-pointing fluctuations within 1-second windows for both directions. The voltage outputs generated from the position sensing detector were digitized by a 24-bit Delta-Sigma analog-to-digital converter (ADC, NI-9202), and the corrected voltages calculated by the FPGA were transmitted to a 16-bit string digital-to-analog converter (DAC, NI-9264). The piezo controller (BPC303, Thorlabs, Inc.) amplifies the corrected voltages 15 times and then directly applies the amplified voltage to the piezo-actuators.

6. Performance Test

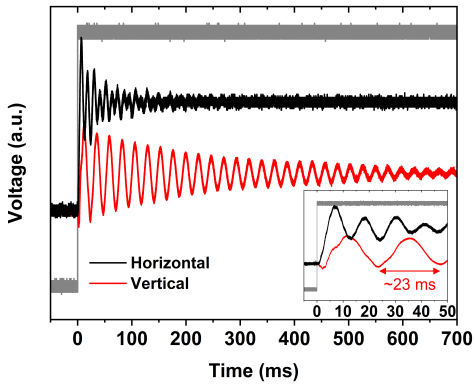

Figure 3. Large-signal step response of the piezo-actuated 16-inch mirror in the horizontal (black) and vertical (red) direction. Grey curve: square wave generated by a function generator. Inset: enlarged view of the first 50 ms.

We simultaneously characterized the ambient vibration on the floor and optical table with the beam-pointing stability measurement using three-dimensional accelerometers. The power spectral density (PSD) of the measured time series is shown in Appendix A, Fig. 7 and 8. The PSD $S(f)$ of a discrete time-series x_n is defined as:

$$S(f) = \frac{\Delta t}{N}\left|\sum_{n=0}^{N-1} x_n \exp\left(-\mathrm{i}2\pi f n \Delta t\right)\right|^2, \qquad (2)$$

where Δt is the sampling interval and N is the total number

https://doi.org/10.1017/hpl.2025.10064 Published online by Cambridge University Press

of samples. The baseline of the ambient vibration on the floor is determined to be 1×10^{-12} g^2/Hz, which is around two orders of magnitude larger than that reported in the ELI-Beamlines[40]. Also, the peak amplitude exceeds the 1×10^{-10} g^2/Hz limit specified by the National Ignition Facility (NIF)[41]. The above-mentioned considerable ambient vibration levels indicate the necessity for most high-power systems to actively compensate for beam-pointing instabilities induced by ambient vibration.

The use of a CW laser provides a more comprehensive picture of beam-pointing instability induced by the home-built 16-inch mirror mount in the frequency domain. In Fig. 2(a) and (b), we show the PSD of the angular deviation sampled at 10 kHz in the horizontal and vertical directions, respectively. Frequencies below 1 Hz dominate both the horizontal and vertical angular deviation. In addition, 33.5 Hz and 44.5 Hz components contribute significantly to the vertical angular deviation. We also observed ∼10 Hz vibrational components on the optical table transferred to the angular deviation in both directions. However, their effects are negligible compared to the frequency components mentioned above. Fig. 2(c) clearly illustrates the significance of each frequency component regarding their contribution to the overall standard deviation of angular beam-pointing fluctuations. The standard deviations of angular pointing fluctuations at different cutoff frequencies are calculated by:

$$\sigma(f_{cutoff}) = \sqrt{\sum_{f_{cutoff}}^{f_{Nyquist}} 2S(f)\Delta f}\ , \tag{3}$$

where σ is the standard deviation, f_{cutoff} is the cutoff frequency, $f_{Nyquist}$ is the Nyquist frequency (50 Hz in this work, except for characterizing the original 16-inch mirror at 10 kHz, where the Nyquist frequency is 5 kHz), $S(f)$ is the PSD as defined in Eq. 2, and $\Delta f = 1/(N\Delta t)$ is the frequency interval.

We determined the cutoff frequencies of the original 16-inch mirror to be 1 Hz and 50 Hz for the horizontal and vertical directions, respectively. The frequency components below the cutoff frequencies contribute to 81% of the total horizontal deviation of 0.796 μrad and 89% of the total vertical deviation of 1.14 μrad.

Fig. 3 shows the large-signal step response of the piezo-actuated 16-inch mirror assembly characterized by a 2.5-GHz oscilloscope. The square wave generated by a function generator was amplified by the piezo controller with a 20-μs rising edge and then drove the piezo-actuators at their maximum drive voltage (150 V). The piezo-actuated 16-inch mirror assembly reached a steady state in the horizontal direction within ∼150 ms. In the vertical direction, the mirror resonates for ∼700 ms with a ∼23 ms period, corresponding to the major peak at 44.5 Hz shown in Fig. 2(b). The 44.5 Hz resonance frequency limits the maximum frequency of beam-pointing instability that could be compensated in our setup; however, this could be mitigated by applying a notch filter at such a frequency in the control algorithm.

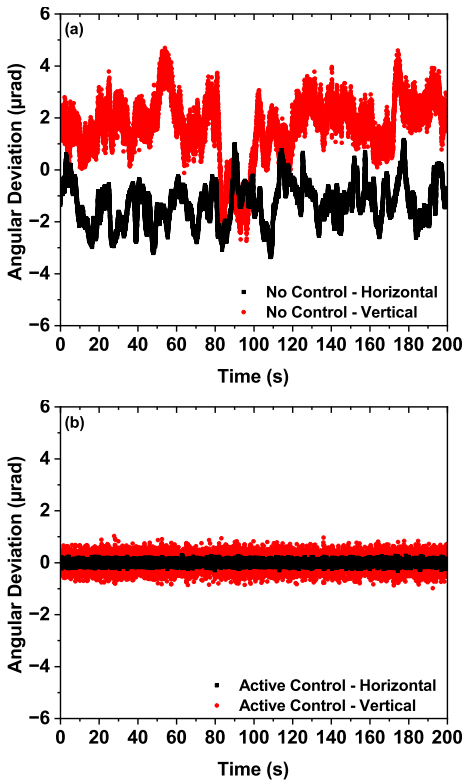

Figure 4. Short-term time series of the beam-pointing in the horizontal (black) and vertical (red) direction sampled at 100 Hz. (a) Piezo-actuated 16-inch mirror without active control. (b) Piezo-actuated 16-inch mirror with active control.

The results of active beam-pointing stabilization with proportional feedback control are shown in Fig. 4. In Fig. 4(a), the driving voltages were kept constant when no control algorithm was implemented. The proportional feedback control was realized at 100 Hz by sampling the position sensing detector's output and driving the piezo-actuators at this frequency. When active control was implemented, the nth sampled beam-pointing deviation was corrected by the (n-1)th sample 10 ms earlier. The feedback loop then acquired the deviation of the nth sample to generate the corrected voltage for the (n+1)th sample. Benefiting from the FPGA architecture, the loop execution time was less than 50 μs without any FPGA optimizations, much less than the sampling interval (10 ms). The loop execution time consists of 8.5 μs ADC input delay, 5.3 μs DAC update time, and 20 μs controller delay during voltage amplification. The standard deviations of the horizontal and vertical angular pointing fluctuations are 0.798 μrad and 1.15 μrad when piezo-actuators are driven at a constant voltage (without active control), consistent with the performance of the original 16-inch mirror without piezo-actuators. This indicates that incorporating the two piezo-actuators does not deteriorate

https://doi.org/10.1017/hpl.2025.10064 Published online by Cambridge University Press

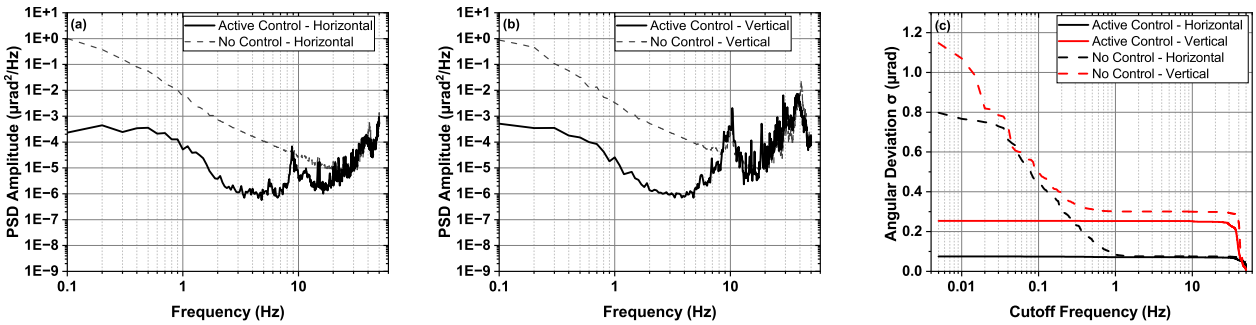

Figure 5. Short-term characterization of the piezo-actuated 16-inch mirror assembly. PSD: power spectral density. (a) Power spectral density of horizontal angular deviation with (solid black) and without (dashed grey) active control. (b) Power spectral density of vertical angular deviation with (solid black) and without (dashed grey) active control. (c) Comparison of the standard deviation of horizontal (black) and vertical (red) angular pointing fluctuations, with only frequencies higher than the cutoff frequency contributing to the standard deviation.

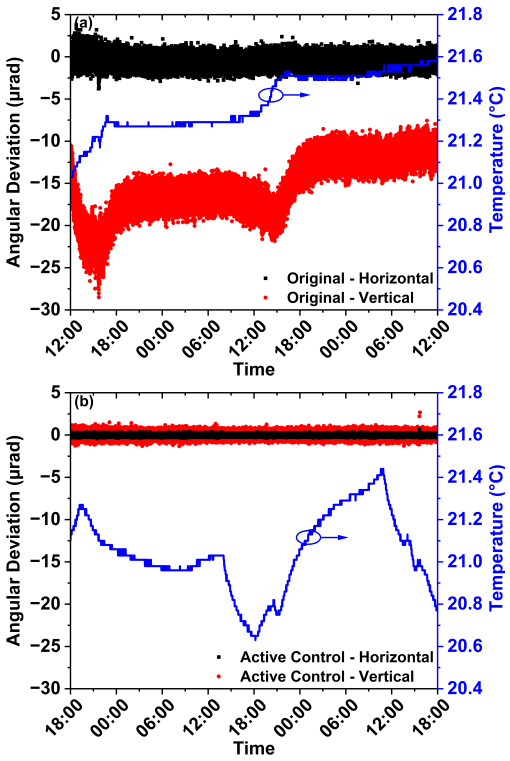

Figure 6. Long-term (48 hours) stability characterization of two 16-inch mirror assemblies in the horizontal (black) and vertical (red) direction. The temperature fluctuation is plotted as the blue curve. (a) Original 16-inch mirror design. (b) Actively controlled piezo-actuated 16-inch mirror assembly.

the mechanical properties of the original 16-mirror assembly design, and the electrical noise of the ADC, DAC, and piezo controllers is negligible. With proportional feedback control, we demonstrated a 91% reduction to 0.0747 μrad in the horizontal direction and a 78% reduction to 0.254 μrad in the vertical direction, as shown in Fig. 4(b). We did not observe significant hysteresis of the piezo-actuators, likely due to the small-signal operating range as a result of the efficacy our control system demonstrated. On the other hand, a feed-forward algorithm could be incorporated to compensate for the actuators' hysteresis[42,43].

To further study the efficacy of the proportional feedback control, we investigated the PSD and cutoff frequency-dependence of the time series of the piezo-actuated 16-inch mirror shown in Fig. 4. The results are shown in Fig. 5. The dashed grey curves shown in Fig. 5(a) and (b) represent the PSD of the angular deviation induced by piezo-actuated mirror without active control and sampled at 100 Hz, which are slightly different from the PSD derived from the characterization of the original 16-inch mirror sampled at 10 kHz (Fig. 2(a) and (b)). With the proportional feedback control, Fig. 5(a) and (b) illustrate at least two orders of magnitude suppression at frequencies lower than ∼5 Hz and more than three orders of magnitude suppression at the low-frequency end in both directions. Fig. 5(c) further demonstrates the efficacy of the active control method by comparing the cutoff frequency-dependent angular deviation with and without proportional feedback control. In the vertical direction, we are able to compensate all the frequency components up to the mirror's resonance frequency at 44.5 Hz. All the frequency components lower than the Nyquist frequency were compensated in the horizontal direction. We believe the small residual in the horizontal direction was due to the convolution of the vertical direction since the laser incident on the mirror at 22.5°.

Managing long-term beam-pointing jitter induced by ambient environmental change is also required for high-power laser systems, since the beam-pointing jitter can significantly

https://doi.org/10.1017/hpl.2025.10064 Published online by Cambridge University Press

deteriorate the experimental results after the initial alignment. As a result, we first studied the beam-pointing jitter of the original 16-inch mirror over 48 hours (Fig. 6(a)). The beam-pointing was sampled at 100 Hz; nonetheless, we only show one point per second for clarity in Fig. 6. We observed a considerable deviation in the vertical direction up to 23 μrad and a 7.6 μrad change in the horizontal direction with only 0.6°C temperature variation. We believe this is due to the difference between the thermal expansion coefficient of the different stainless steel components, which is the material of both our customized and off-the-shelf parts. The original 16-inch mirror assembly experienced relaxation and re-equilibrium during the temperature changes. We completely eliminated the long-term beam-pointing jitter with the same proportional feedback control operating at 100 Hz, as shown in Fig. 6(b). With a larger temperature variation of 0.8°C and more random fluctuation, the standard deviation of the horizontal and vertical beam-pointing jitter is reduced to 0.085 μrad and 0.29 μrad, respectively. The long-term stabilization results further demonstrate the robustness of our control method.

7. Conclusion

In summary, we demonstrated an actively controlled 16-inch mirror in a high-power laser system. Active control of the beam-pointing with large optics is of vital importance for a wide range of experiments facilitated with a high-power laser system such as ZEUS. With two piezo-actuators and a simple FPGA-based proportional feedback control, we reduced the short-term beam-pointing instability by up to an order of magnitude, from (0.798, 1.15) to (0.0747, 0.254) μrad in the (horizontal, vertical) direction, providing an adequate margin from the beam-pointing requirement of a few μrad. The long-term drift due to temperature variation was also eliminated. Given the considerable baseline of ambient vibration reported in the ZEUS facility, our approach manifests its effectiveness, although it is limited by the resonance frequency of the optics assembly, which could be mitigated by implementing a notch filter in the control algorithm. To integrate the presented active beam-pointing control system in the ZEUS system, an online and non-destructive diagnostic at the focus[35] of a PW-class laser is necessary and can be challenging to implement. A mechanical shutter with a few-millisecond close time is also needed to block the amplified beam from the diagnostics so that the position sensing detector only detects the unamplified beam after proper attenuation.

It would be beneficial in future work to fine-tune the resonance frequency of the 16-inch mirror assembly to a frequency higher than the Nyquist frequency of the active control system, assisted by FEA. With such a mechanical design improvement, our proportional feedback control could potentially compensate for beam-pointing instabilities up to the Nyquist frequency, which is 50 Hz in the scheme described in this work. The performance of the control system could be improved by analyzing and optimizing its frequency response and gain using a mathematical model and incorporating integral and derivative terms into the feedback loop. Data-driven Recurrent Neural Network models such as Long Short-Term Memory and Gated Recurrent Unit could also be employed to improve the efficacy of the feedback control[44,45]. However, a substantial amount of data from the actual laser shots must be collected to train such models.

Acknowledgement

We acknowledge support from the US National Science Foundation Mid-scale Research Award 1935950 and the US Department of Energy grant DE-SC0016804.

A. Ambient vibration measured in the ZEUS facility

The ambient vibration on the floor and optical table in the ZEUS facility were simultaneously characterized along the beam-pointing stability measurement using three-dimensional accelerometers. The standard deviations of the ambient vibration on the floor in the x, y, and z directions are 2.41×10^{-4} g, 1.65×10^{-4} g, and 2.10×10^{-4} g, respectively. Whereas the values are increased to 2.77×10^{-4} g, 1.83×10^{-4} g, and 3.02×10^{-4} g on the optical table. As shown in Fig. 8, in the horizontal directions x (perpendicular to the main laser chain) and y (parallel to the main laser chain), frequencies below 2 Hz, at 9 Hz and 60 Hz, are prominent in the PSD below 100 Hz. We aim our attention at frequency components lower than 100 Hz due to the $1/f^2$ scaling law for displacement regarding the frequency. Other laser facilities have also identified a cutoff frequency lower than 100 Hz (See, for example, Ref.[35,37]). The 30 Hz component in the y-direction also contributes significantly. In the z-direction (vertical to the table surface), a broader frequency range between 14 and 83 Hz has a significant contribution in addition to the frequencies below 2 Hz.

References

1. Ahmed H Zewail. “Femtochemistry: Atomic-scale dynamics of the chemical bond”. In: *The Journal of Physical Chemistry A* 104.24 (2000), pp. 5660–5694.
2. Bruce A Remington, R Paul Drake, and Dmitri D Ryutov. “Experimental astrophysics with high power lasers and Z pinches”. In: *Reviews of Modern Physics* 78.3 (2006), p. 755.
3. SV Bulanov, T Zh Esirkepov, D Habs, F Pegoraro, and T Tajima. “Relativistic laser-matter interaction and relativistic laboratory astrophysics”. In: *The European Physical Journal D* 55 (2009), pp. 483–507.

https://doi.org/10.1017/hpl.2025.10064 Published online by Cambridge University Press

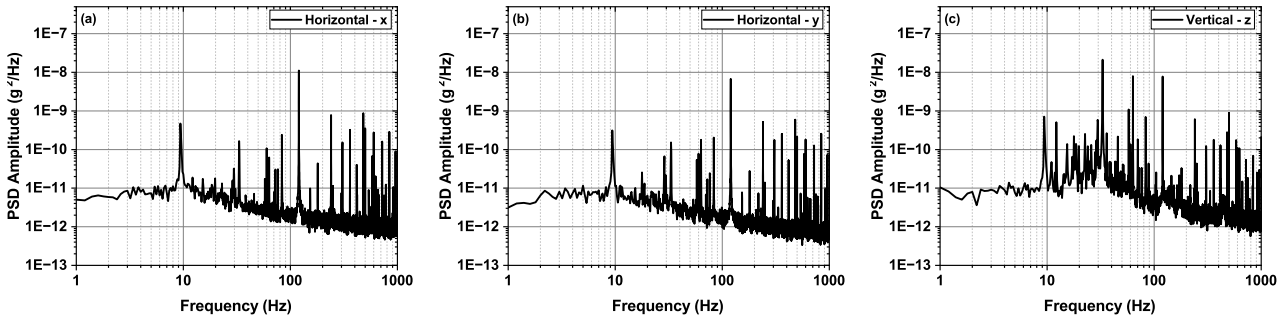

Figure 7. Ambient vibration measured on the floor near the 3-PW compressor in the ZEUS facility. PSD: power spectral density. (a) Horizontal direction perpendicular to the main laser chain. (b) Horizontal direction parallel to the main laser chain. (c) Vertical direction.

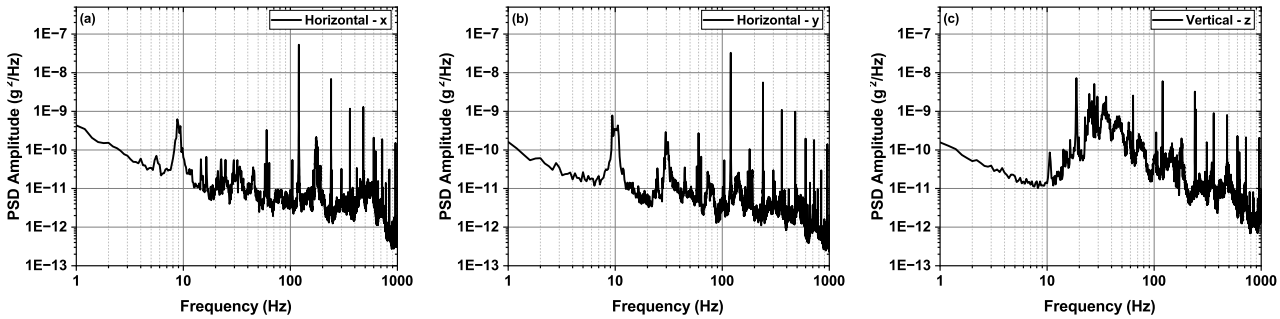

Figure 8. Ambient vibration measured on the optical table of the main laser chain in the ZEUS facility. PSD: power spectral density. (a) Horizontal direction perpendicular to the main laser chain. (b) Horizontal direction parallel to the main laser chain. (c) Vertical direction.

4. D Habs, T Tajima, J Schreiber, CPJ Barty, M Fujiwara, and PG Thirolf. “Vision of nuclear physics with photonuclear reactions by laser-driven beams”. In: *The European Physical Journal D* 55.2 (2009), p. 279.

5. AB Zylstra, OA Hurricane, DA Callahan, AL Kritcher, JE Ralph, HF Robey, JS Ross, CV Young, KL Baker, DT Casey, T Döppner, L Divol, M Hohenberger, S Le Pape, A Pak, PK Patel, R Tommasini, SJ Ali, PA Amendt, LJ Atherton, B Bachmann, D Bailey, LR Benedetti, L Berzak Hopkins, R Betti, SD Bhandarkar, J Biener, RM Bionta, NW Birge, EJ Bond, DK Bradley, T Braun, TM Briggs, MW Bruhn, PM Celliers, B Chang, T Chapman, H Chen, C Choate, AR Christopherson, DS Clark, JW Crippen, EL Dewald, TR Dittrich, MJ Edwards, WA Farmer, JE Field, D Fittinghoff, J Frenje, J Gaffney, M Gatu Johnson, SH Glenzer, GP Grim, S Haan, KD Hahn, GN Hall, BA Hammel, J Harte, E Hartouni, JE Heebner, VJ Hernandez, H Herrmann, MC Herrmann, DE Hinkel, DD Ho, JP Holder, WW Hsing, H Huang, KD Humbird, N Izumi, LC Jarrott, J Jeet, O Jones, GD Kerbel, SM Kerr, SF Khan, J Kilkenny, Y Kim, H Geppert Kleinrath, V Geppert Kleinrath, C Kong, JM Koning, JJ Kroll, MKG Kruse, B Kustowski, OL Landen, S Langer, D Larson, NC Lemos, JD Lindl, T Ma, MJ MacDonald, BJ MacGowan, AJ Mackinnon, SA MacLaren, AG MacPhee, MM Marinak, DA Mariscal, EV Marley, L Masse, K Meaney, NB Meezan, PA Michel, M Millot, JL Milovich, JD Moody, AS Moore, JW Morton, T Murphy, K Newman, JMG Di Nicola, A Nikroo, R Nora, MV Patel, LJ Pelz, JL Peterson, Y Ping, BB Pollock, M Ratledge, NG Rice, H Rinderknecht, M Rosen, MS Rubery, JD Salmonson, J Sater, S Schiaffino, DJ Schlossberg, MB Schneider, CR Schroeder, HA Scott, SM Sepke, K Sequoia, MW Sherlock, S Shin, VA Smalyuk, BK Spears, PT Springer, M Stadermann, S Stoupin, DJ Strozzi, LJ Suter, CA Thomas, RPJ Town, ER Tubman, C Trosseille, PL Volegov, CR Weber, K Widmann, C Wild, CH Wilde, BM Van Wonterghem, DT Woods, BN Woodworth, M Yamaguchi, ST Yang, and GB Zimmerman. “Burning plasma achieved in inertial fusion”. In: *Nature* 601.7894 (2022), pp. 542–548.

6. Toshiki Tajima and John M Dawson. “Laser electron accelerator”. In: *Physical Review Letters* 43.4 (1979), p. 267.

7. C GR Geddes, Cs Toth, J van Tilborg, E Esarey, CB Schroeder, D Bruhwiler, C Nieter, J Cary, and WP Leemans. “High quality electron beams from a plasma channel guided laser wakefield accelerator”. In: *Nature* 431.7008 (2004).

https://doi.org/10.1017/hpl.2025.10064 Published online by Cambridge University Press

8. SP Mangles, CD Murphy, Z Najmudin, AGR Thomas, JL Collier, AE Dangor, EJ Divall, PS Foster, JG Gallacher, CJ Hooker, DA Jaroszynski, AJ Langley, WB Mori, PA Norreys, FS Tsung, R Viskup, BR Walton, and K Krushelnick. "Monoenergetic beams of relativistic electrons from intense laser-plasma interactions". In: *Nature* 431.7008 (2004), pp. 535–538.
9. Jérôme Faure, Yannick Glinec, A Pukhov, S Kiselev, S Gordienko, E Lefebvre, J-P Rousseau, F Burgy, and Victor Malka. "A laser-plasma accelerator producing monoenergetic electron beams". In: *Nature* 431.7008 (2004), pp. 541–544.
10. Wim P Leemans, Bob Nagler, Anthony J Gonsalves, Cs Tóth, Kei Nakamura, Cameron GR Geddes, ESCB Esarey, CB Schroeder, and SM Hooker. "GeV electron beams from a centimetre-scale accelerator". In: *Nature Physics* 2.10 (2006), pp. 696–699.
11. Wei Lu, M Tzoufras, C Joshi, FS Tsung, WB Mori, J Vieira, RA Fonseca, and LO Silva. "Generating multi-GeV electron bunches using single stage laser wakefield acceleration in a 3D nonlinear regime". In: *Physical Review Special Topics-Accelerators and Beams* 10.6 (2007), p. 061301.
12. Eric Esarey, Carl B Schroeder, and Wim P Leemans. "Physics of laser-driven plasma-based electron accelerators". In: *Reviews of modern physics* 81.3 (2009), p. 1229.
13. Andrea Macchi, Marco Borghesi, and Matteo Passoni. "Ion acceleration by superintense laser-plasma interaction". In: *Reviews of Modern Physics* 85.2 (2013), p. 751.
14. Xing-Long Zhu, Min Chen, Su-Ming Weng, Tong-Pu Yu, Wei-Min Wang, Feng He, Zheng-Ming Sheng, Paul McKenna, Dino A Jaroszynski, and Jie Zhang. "Extremely brilliant GeV γ-rays from a two-stage laser-plasma accelerator". In: *Science Advances* 6.22 (2020), eaaz7240.
15. JM Cole, KT Behm, E Gerstmayr, TG Blackburn, JC Wood, CD Baird, MJ Duff, C Harvey, A Ilderton, AS Joglekar, K Krushelnick, S Kuschel, M Marklund, P McKenna, CD Murphy, K Poder, CP Ridgers, GM Samarin, G Sarri, DR Symes, AGR Thomas, J Warwick, M Zepf, Z Najmudin, and SPD Mangles. "Experimental evidence of radiation reaction in the collision of a high-intensity laser pulse with a laser-wakefield accelerated electron beam". In: *Physical Review X* 8.1 (2018), p. 011020.
16. K Poder, M Tamburini, G Sarri, A Di Piazza, S Kuschel, CD Baird, K Behm, S Bohlen, JM Cole, DJ Corvan, M Duff, E Gerstmayr, CH Keitel, K Krushelnick, SPD Mangles, P McKenna, CD Murphy, Z Najmudin, CP Ridgers, GM Samarin, DR Symes, AGR Thomas, J Warwick, and M Zepf. "Experimental signatures of the quantum nature of radiation reaction in the field of an ultraintense laser". In: *Physical Review X* 8.3 (2018), p. 031004.
17. S-W Bahk, Pascal Rousseau, TA Planchon, Vladimir Chvykov, Galina Kalintchenko, Anatoly Maksimchuk, GA Mourou, and Victor Yanovsky. "Generation and characterization of the highest laser intensities (10^{22} W/cm^2)". In: *Optics Letters* 29.24 (2004), pp. 2837–2839.
18. Jin Woo Yoon, Cheonha Jeon, Junghoon Shin, Seong Ku Lee, Hwang Woon Lee, Il Woo Choi, Hyung Taek Kim, Jae Hee Sung, and Chang Hee Nam. "Achieving the laser intensity of 5.5×10^{22} W/cm^2 with a wavefront-corrected multi-PW laser". In: *Optics Express* 27.15 (2019), pp. 20412–20420.
19. Jin Woo Yoon, Yeong Gyu Kim, Il Woo Choi, Jae Hee Sung, Hwang Woon Lee, Seong Ku Lee, and Chang Hee Nam. "Realization of laser intensity over 10^{23} W/cm^2". In: *Optica* 8.5 (2021), pp. 630–635.
20. J Nees, A Maksimchuk, G Kalinchenko, B Hou, Y Ma, P Campbell, A McKelvey, L Willingale, I Jovanovic, C Kuranz, A Thomas, and K Krushelnick. "Zettawatt Equivalent Ultrashort pulse laser System: An NSF mid-scale facility for laser-driven science in the QED regime". In: *CLEO: Science and Innovations*. Optica Publishing Group. 2021, JTu3A–10.
21. L Willingale, A Maksimchuk, J Nees, F Bayer, M Burger, PT Campbell, B Hou, I Jovanovic, G Kalinchenko, CC Kuranz, Y Ma, A McKelvey, AGR Thomas, L Weinberg, Q Zhang, and K Krushelnick. "Status of the ZEUS laser user facility". In: *CLEO: Science and Innovations*. Optica Publishing Group. 2023, SM1D–7.
22. P Zhang, SS Bulanov, D Seipt, AV Arefiev, and AGR Thomas. "Relativistic plasma physics in supercritical fields". In: *Physics of Plasmas* 27.5 (2020), p. 050601.
23. A Gonoskov, TG Blackburn, M Marklund, and SS Bulanov. "Charged particle motion and radiation in strong electromagnetic fields". In: *Reviews of Modern Physics* 94.4 (2022), p. 045001.
24. A Fedotov, A Ilderton, F Karbstein, Ben King, D Seipt, H Taya, and Greger Torgrimsson. "Advances in QED with intense background fields". In: *Physics Reports* 1010 (2023), pp. 1–138.
25. Jérôme Faure, Clément Rechatin, A Norlin, Agustin Lifschitz, Y Glinec, and Victor Malka. "Controlled injection and acceleration of electrons in plasma wakefields by colliding laser pulses". In: *Nature* 444.7120 (2006), pp. 737–739.

https://doi.org/10.1017/hpl.2025.10064 Published online by Cambridge University Press

26. A Popp, J Vieira, J Osterhoff, Z Major, R Hörlein, M Fuchs, R Weingartner, TP Rowlands-Rees, M Marti, RA Fonseca, SF Martins, LO Silva, SM Hooker, F Krausz, F Grüner, and S Karsch. "All-optical steering of laser-wakefield-accelerated electron beams". In: *Physical review letters* 105.21 (2010), p. 215001.

27. Y Ma, D Seipt, SJD Dann, MJV Streeter, CAJ Palmer, L Willingale, and AGR Thomas. "Angular streaking of betatron X-rays in a transverse density gradient laser-wakefield accelerator". In: *Physics of Plasmas* 25.11 (2018).

28. Jacob Pieter Den Hartog. *Mechanical vibrations*. Courier Corporation, 1985.

29. Byoung-Uk Nam, Hakin Gimm, Dongwoo Kang, and Daegab Gweon. "Design and analysis of a tip–tilt guide mechanism for the fast steering of a large-scale mirror". In: *Optical Engineering* 55.10 (2016), pp. 106120–106120.

30. Shane Woody and Stuart Smith. "Design and performance of a dual drive system for tip-tilt angular control of a 300 mm diameter mirror". In: *Mechatronics* 16.7 (2006), pp. 389–397.

31. John T Stein and Conrad Neufeld. "A fast steering tertiary mirror for the SOAR telescope". In: *Astronomical Structures and Mechanisms Technology*. Vol. 5495. SPIE. 2004, pp. 340–347.

32. Takuya Kanai, Akira Suda, Samuel Bohman, Masanori Kaku, Shigeru Yamaguchi, and Katsumi Midorikawa. "Pointing stabilization of a high-repetition-rate high-power femtosecond laser for intense few-cycle pulse generation". In: *Applied Physics Letters* 92.6 (2008), p. 061106.

33. Robert A Hardin, Yun Liu, Cary Long, Alexander Aleksandrov, and Willem Blokland. "Active beam position stabilization of pulsed lasers for long-distance ion profile diagnostics at the Spallation Neutron Source (SNS)". In: *Optics Express* 19.4 (2011), pp. 2874–2885.

34. Guillaume Genoud, Franck Wojda, Matthias Burza, Anders Persson, and C-G Wahlström. "Active control of the pointing of a multi-terawatt laser". In: *Review of Scientific Instruments* 82.3 (2011), p. 033102.

35. Fumika Isono, Jeroen van Tilborg, Samuel K Barber, Joseph Natal, Curtis Berger, Hai-En Tsai, Tobias Ostermayr, Anthony Gonsalves, Cameron Geddes, and Eric Esarey. "High-power non-perturbative laser delivery diagnostics at the final focus of 100-TW-class laser pulses". In: *High Power Laser Science and Engineering* 9 (2021), e25.

36. Martin J Kay, Abdurahim A Rakhman, and Sarah M Cousineau. "Active pointing control of pulsed, high-power laser beam after 65-meter transport". In: *2022 IEEE 17th International Conference on Control & Automation (ICCA)*. IEEE. 2022, pp. 565–570.

37. Shunxing Tang, Yajing Guo, Pengqian Yang, Xiuqing Jiang, Neng Hua, and Nan Zong. "Stability improvement of multi-beam picosecond-petawatt laser system for ultrahigh peak-power applications". In: *Frontiers in Physics* 11 (2023), p. 1118254.

38. Curtis Berger, Sam Barber, Fumika Isono, Kyle Jensen, Joseph Natal, Anthony Gonsalves, and Jeroen van Tilborg. "Active nonperturbative stabilization of the laser-plasma-accelerated electron beam source". In: *Physical Review Accelerators and Beams* 26.3 (2023), p. 032801.

39. PI (Physik Instrumente) L.P. *S-340 Piezo Tip/Tilt Platform*. 2023. URL: https://www.pi-usa.us/en/products/fast-steering-mirrors-fsm-and-piezo-tiptilt-platforms-for-active-optics/s-340-piezo-tip-tilt-platform-300811.

40. S Borneis, T Laštovička, M Sokol, TM Jeong, F Condamine, O Renner, V Tikhonchuk, H Bohlin, A Fajstavr, JC Hernandez, N Jourdain, D Kumar, D Modřanský, A Pokorný, A Wolf, S Zhai, G Korn, and S Weber. "Design, installation and commissioning of the ELI-Beamlines high-power, high-repetition rate HAPLS laser beam transport system to P3". In: *High Power Laser Science and Engineering* 9 (2021), e30.

41. David J Trummer, Richard J Foley, and Gene S Shaw. "Stability of optical elements in the NIF target area building". In: *Third International Conference on Solid State Lasers for Application to Inertial Confinement Fusion*. Vol. 3492. SPIE. 1999, pp. 363–371.

42. Fangbo Qin, Dapeng Zhang, Dengpeng Xing, De Xu, and Jianquan Li. "Laser beam pointing control with piezoelectric actuator model learning". In: *IEEE Transactions on Systems, Man, and Cybernetics: Systems* 50.3 (2017), pp. 1024–1034.

43. Joseph Natal, Samuel Barber, Fumika Isono, Curtis Berger, Anthony J Gonsalves, Matthias Fuchs, and Jeroen van Tilborg. "High-bandwidth image-based predictive laser stabilization via optimized Fourier filters". In: *Applied Optics* 62.2 (2023), pp. 440–446.

44. F Breitling, RS Weigel, MC Downer, and T Tajima. "Laser pointing stabilization and control in the submicroradian regime with neural networks". In: *Review of Scientific Instruments* 72.2 (2001), pp. 1339–1342.

45. Hui Chang, Wen-Qi Ge, Hao-Cheng Wang, Hong Yuan, and Zhong-Wei Fan. "Laser beam pointing stabilization control through disturbance classification". In: *Sensors* 21.6 (2021), p. 1946.

https://doi.org/10.1017/hpl.2025.10064 Published online by Cambridge University Press